

Exotic Forms of Superconductivity

- Excitonic SC
- Spin-polarized SC
- Finite-momentum SC

Collaboration



Max Geier



Margarita Davydova
(=>Caltech)

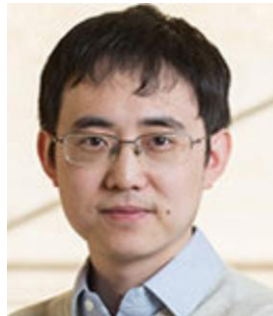


Filippo Gaggioli



Daniele Guerci

Experiment:



Long Ju



Tonghang Han

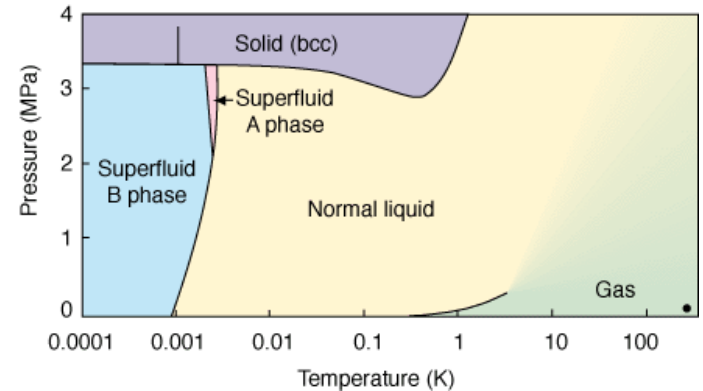


Spin-Singlet vs Spin-Triplet



$$\psi(r_1, r_2) | \uparrow\downarrow - \downarrow\uparrow \rangle$$

with $\psi(r_1, r_2) = \psi(r_2, r_1)$



$$\psi_+(r_1, r_2) | \uparrow\uparrow \rangle + \psi_-(r_1, r_2) | \downarrow\downarrow \rangle + \psi_0(r_1, r_2) | \uparrow\downarrow - \downarrow\uparrow \rangle$$

with $\psi_a(r_1, r_2) = -\psi_a(r_2, r_1)$

Almost all known SCs are spin-singlet and even-parity.

Search for Spin-Triplet Superconductor

Lesson from Sr_2RuO_4 :

Letter | Published: 17 December 1998

Spin-triplet superconductivity in Sr_2RuO_4 identified by ^{17}O Knight shift

Letter | Published: 23 September 2019

Constraints on the superconducting order parameter in Sr_2RuO_4 from oxygen-17 nuclear magnetic resonance

Perspective | Published: 11 November 2024

Thirty years of puzzling superconductivity in Sr_2RuO_4

Spin-Polarized SC

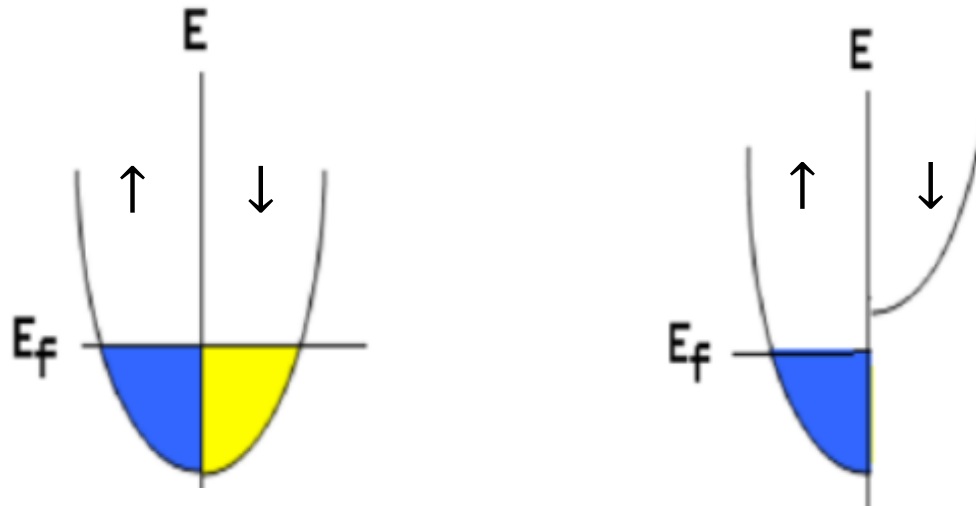


$$\psi(r_1, r_2) | \uparrow\uparrow \rangle \quad \text{with } \psi(r_1, r_2) = -\psi(r_2, r_1)$$

SC in fully spin-polarized metal must be odd-parity, e.g., p- or f-wave.

Full SP can be induced by magnetic field, e.g., in twisted TMD.

Half Metal

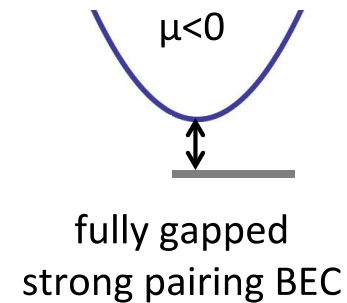
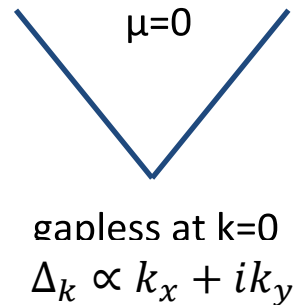
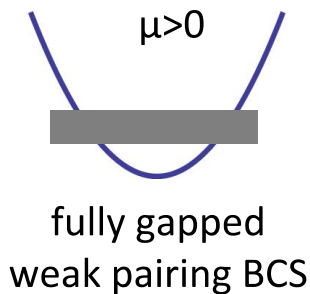


Stoner ferromagnetism may lead to 100% spin polarization at Fermi level.

Until recently no known half metals are superconducting.

Topological Superconductivity

BCS and BEC phases of a p-wave SC can be *topologically* distinct, in contrast to the case of s-wave SC.



- Quasiparticle gap closes and re-opens across p-wave BCS/BEC transition, indicating a change in topology.

$$E_k = \sqrt{(\epsilon_k - \mu)^2 + \Delta_k^2}$$

Read & Green (2000)

Majorana Fermions

In BEC state, there exists finite energy gap to fermionic excitations anywhere, either bulk or boundary.

In topological BCS state, there is a gap to fermionic excitations in the bulk, but the boundary hosts gapless Majorana fermions

$$\gamma = \gamma^+ \sim c + c^+.$$

Read & Green (2000), Kitaev (2000)

boundary of a topological state

= domain wall between topologically distinct states

That change in topology requires gap closing implies the existence of gapless excitations at the domain wall.

Rhombohedral Graphene

Article | Published: 01 September 2021

Half- and quarter-metals in rhombohedral trilayer graphene

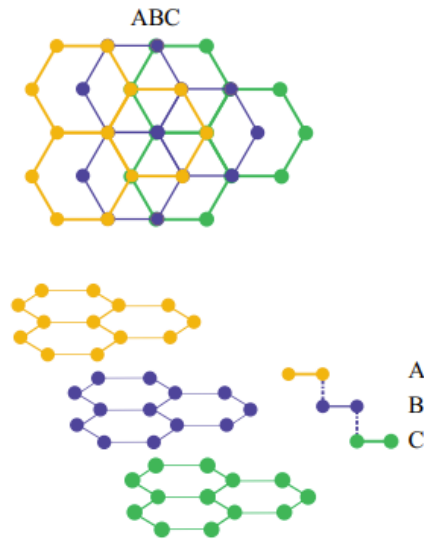
Article | Published: 01 September 2021

Superconductivity in rhombohedral trilayer graphene

Andrea Young's group

Rhombohedral Graphene

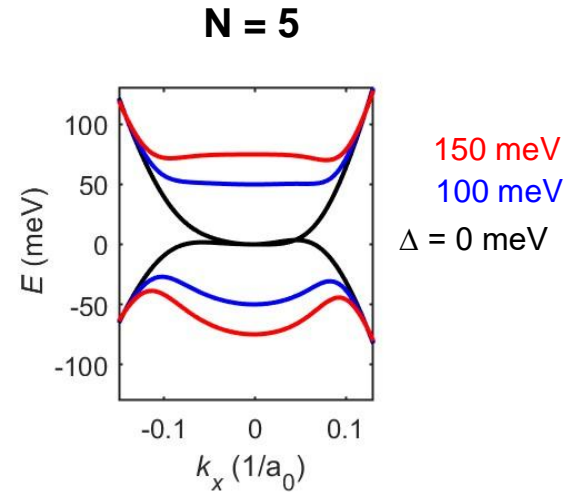
Stacking: ABCA...



large DOS & Berry curvature
strong correlation & topology

H. Min and A. H. MacDonald, *PRB* (2008)

F. Zhang et al. *PRB* (2010)



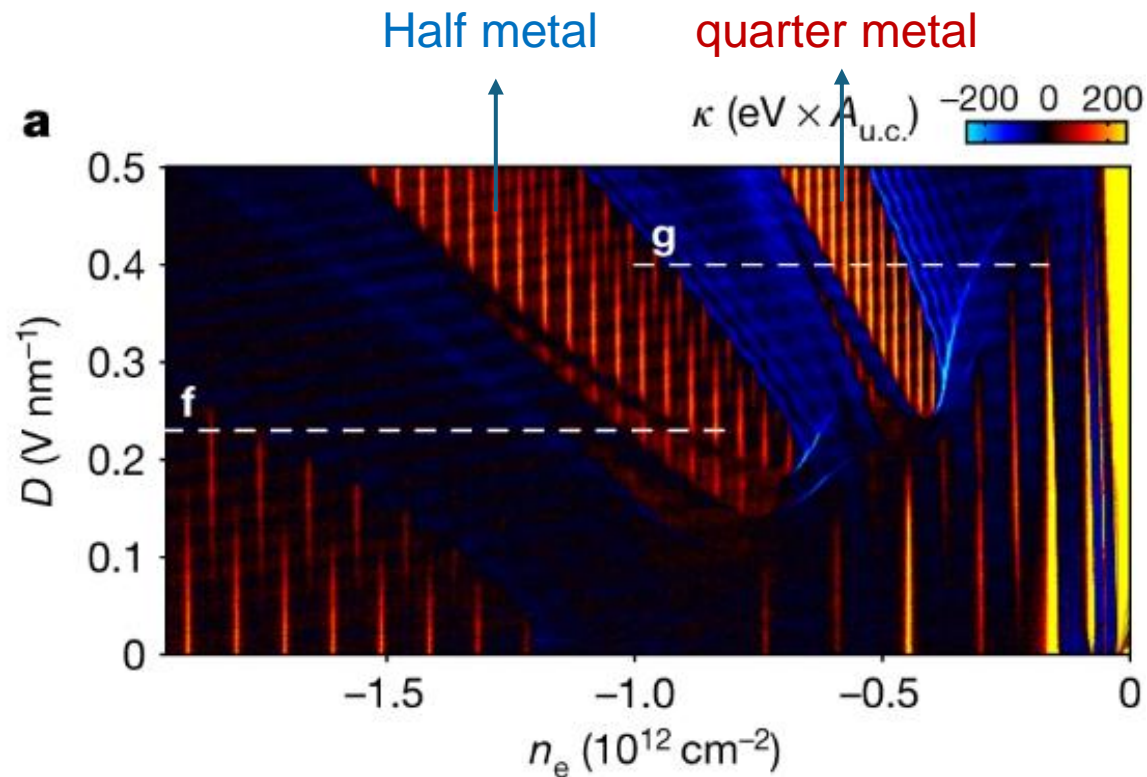
$$H_N = \begin{pmatrix} \Delta/2 & (k_x - ik_y)^N \\ (k_x + ik_y)^N & -\Delta/2 \end{pmatrix}$$

Gate tunable band gap: $\Delta \sim E^*d$

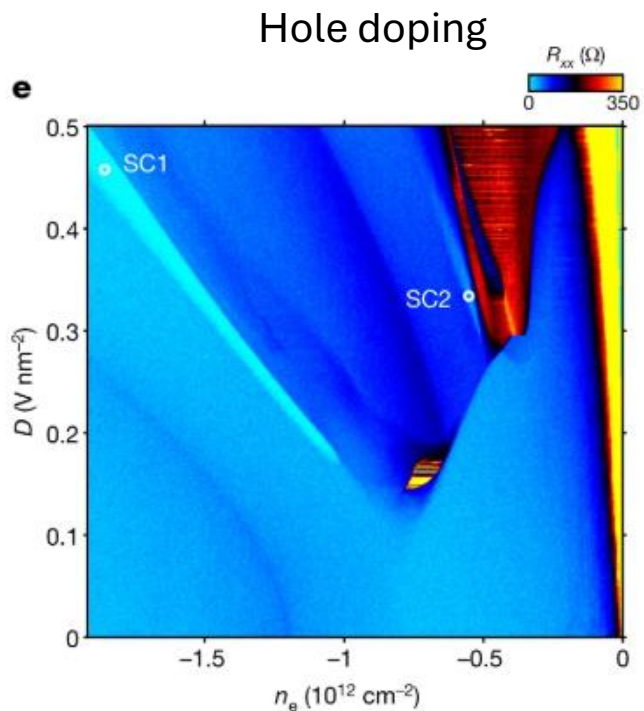
Low energy dispersion: $\varepsilon \sim \pm (\Delta/2 + |k|^{2N})$

Half and Quarter Metal

Spin and valley degeneracy is spontaneously broken at low density and large displacement field due to interaction effect.



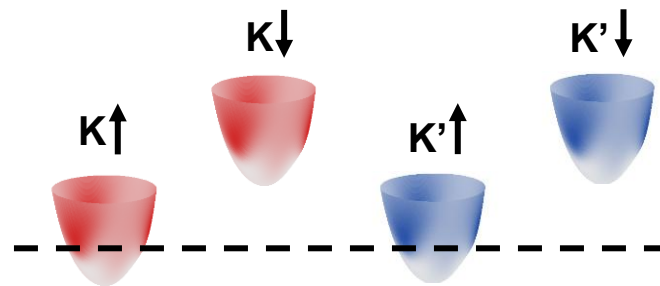
Superconductivity in Trilayer RG



Zhou .. Young, Nature (2021)

SC1 emerges from a paramagnetic normal state.

SC2 emerges from a spin-polarized, valley-unpolarized **half-metal**

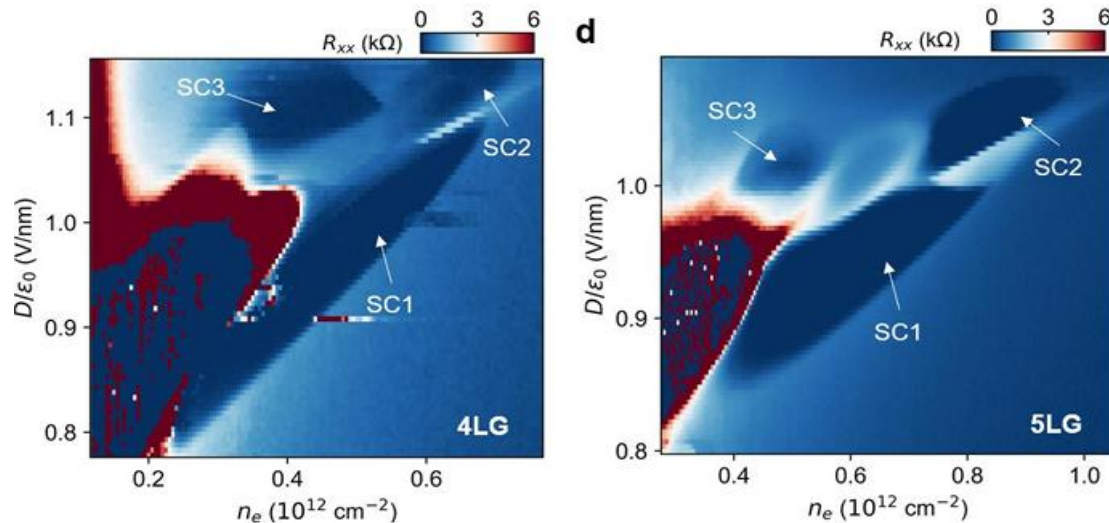


Candidate: spin-triplet, valley-singlet (f-wave) SC

- compatible with spinless T symmetry
- excitonic mechanism?

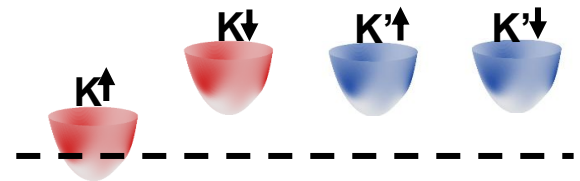
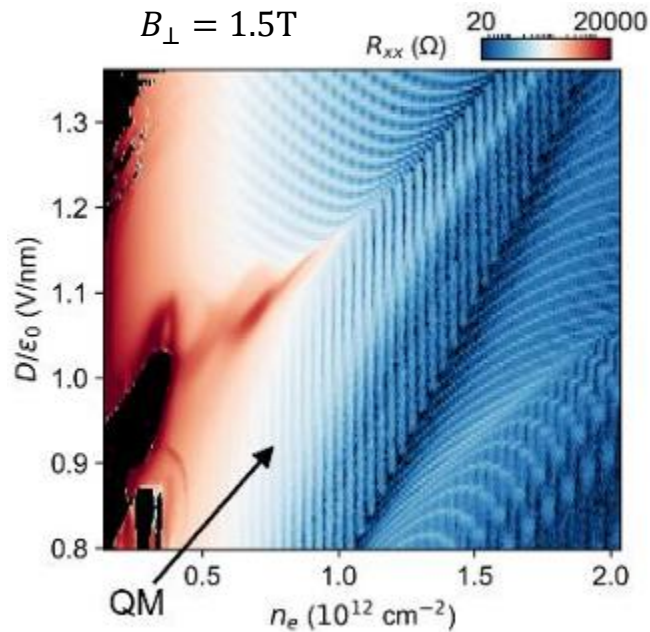
New & Different: SC in Tetra- and Penta-layers

electron doping



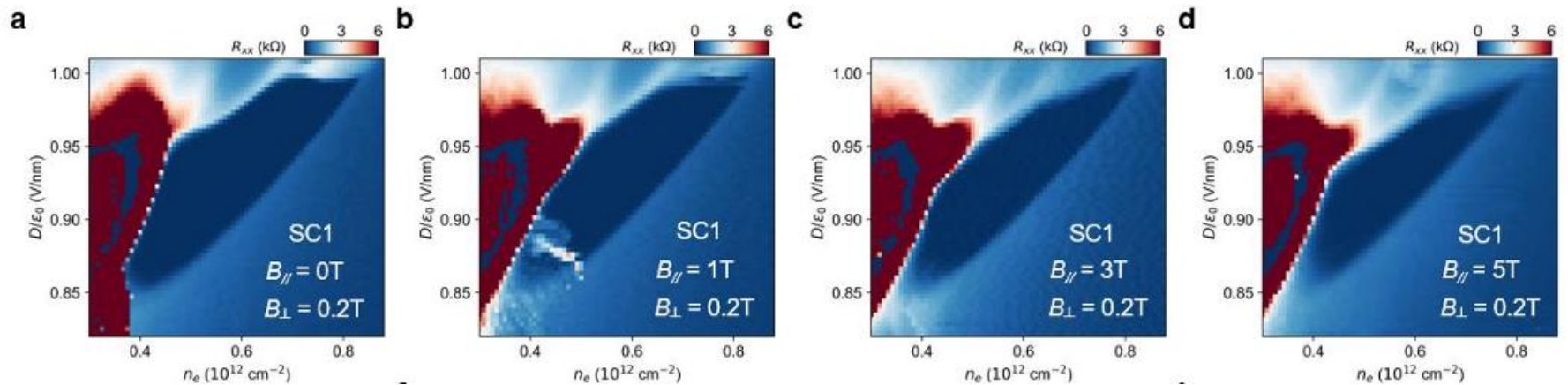
- SC1 & SC2 emerge from spin- and valley-polarized **quarter-metal**.
- SC1 is adjacent to Wigner crystal at lower density.

Spin- & Valley-Polarized Superconductivity



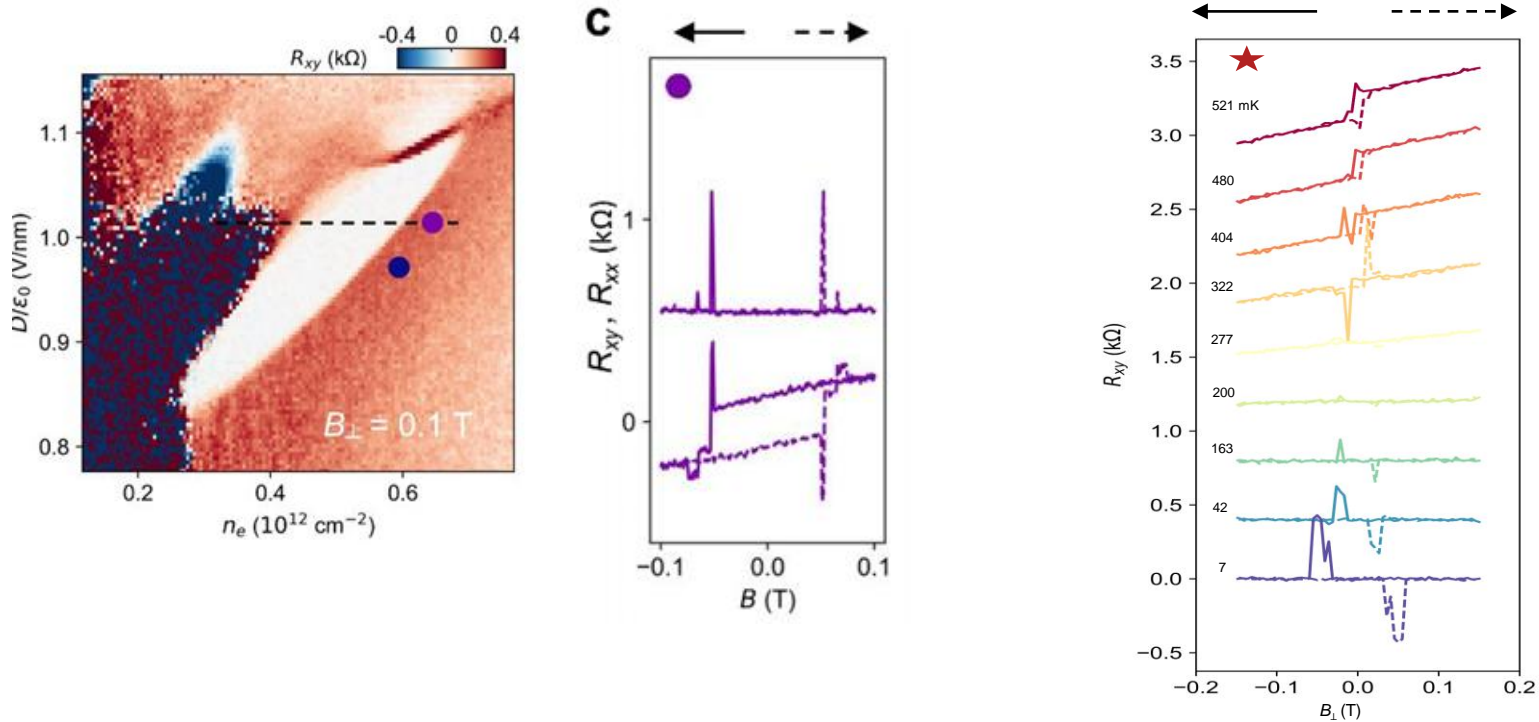
- Quantum oscillation shows quarter metal, i.e., spin and valley degeneracy are completely lifted

Spin- & Valley-Polarized Superconductivity



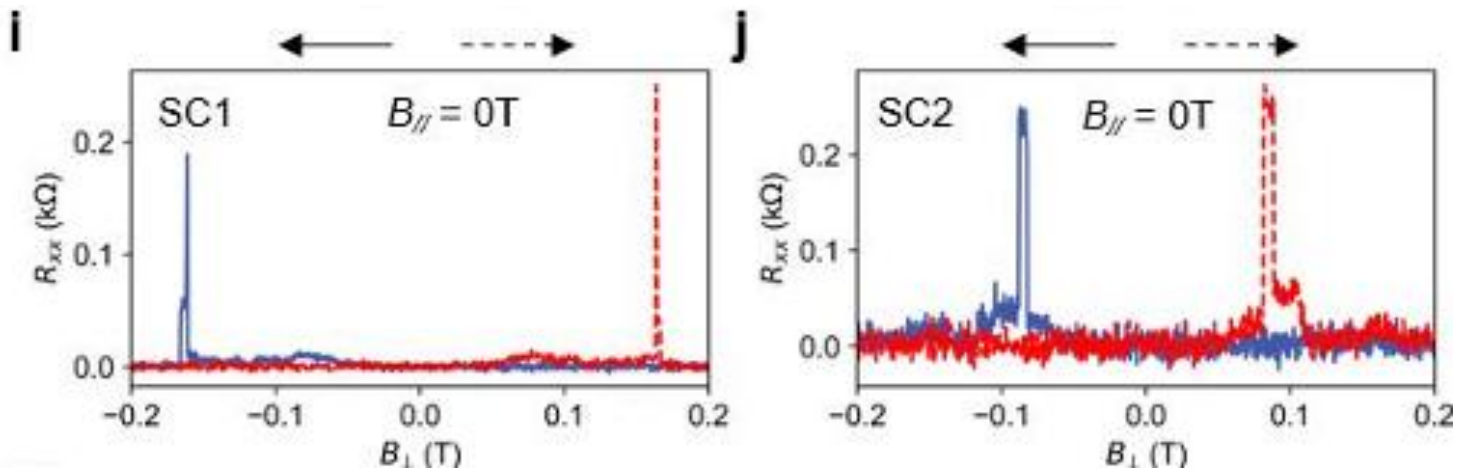
- Quantum oscillation shows quarter metal
- SC1 & SC2 survive $B_{//}$ at least up to 5T ($\sim 15B_{\text{Pauli}}$)

Spin- & Valley-Polarized Superconductivity

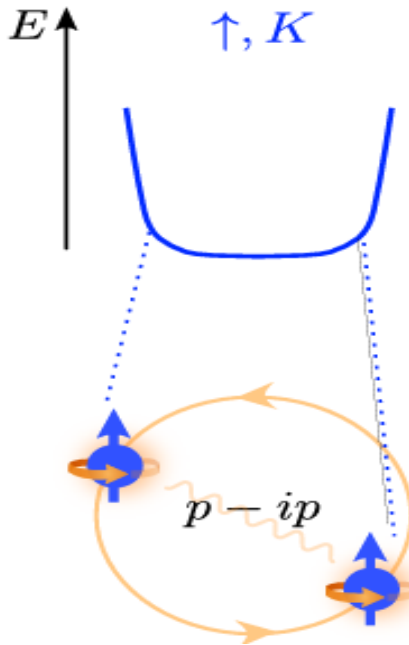


- Quantum oscillation shows quarter metal
- SC1 & SC2 survive $B_{//}$ at least up to 5T ($\sim 15B_{\text{Pauli}}$)
- **AHE above T_c** \Rightarrow valley polarization

A Superconductor AND a Magnet

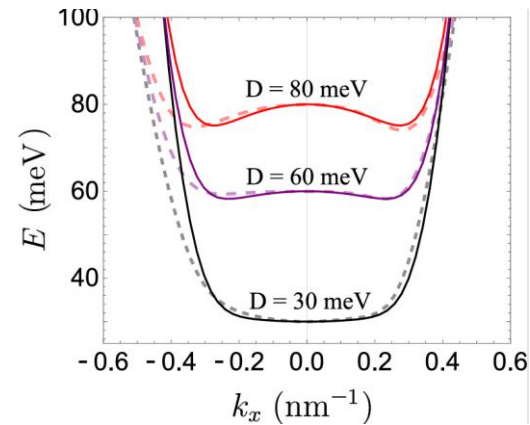
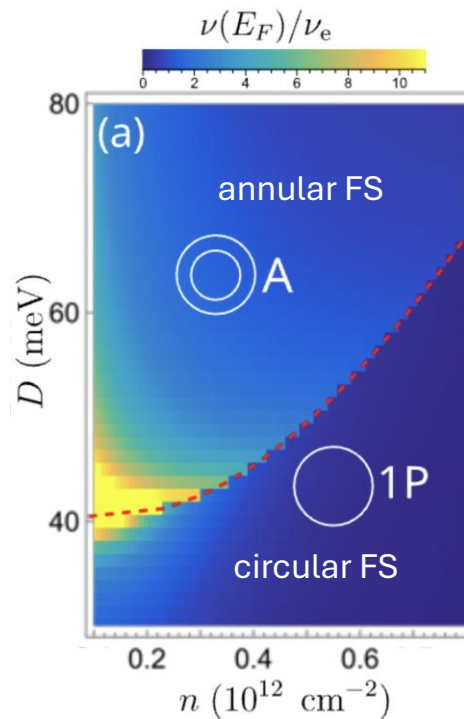


Intra-valley Pairing



- Cooper pair momentum $Q \sim 2K$
- Pauli principle dictates odd-parity pairing
- Pairing mechanism and symmetry ?
- Effects of time-reversal-breaking ?
- Topological ?
- Intertwining phases ?

Phase Diagram

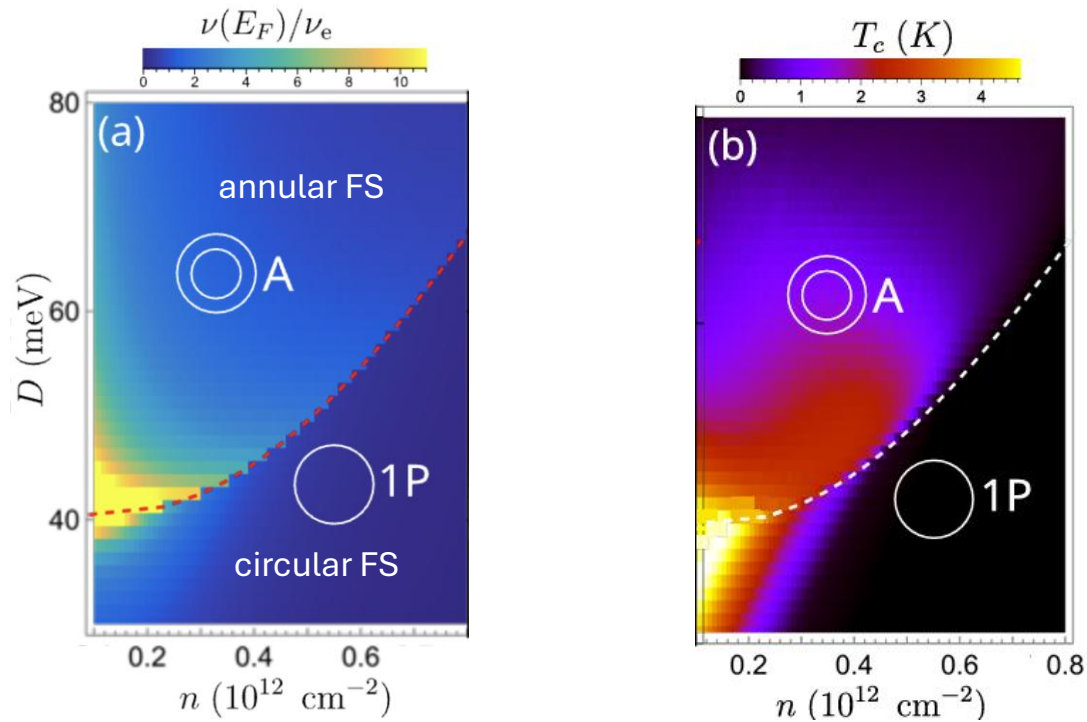


Displacement field drives Lifshitz transition from circular to annular Fermi sea.

Minimal model (without trigonal warping):

$$\varepsilon_k = D\sqrt{1 + (k/k_0)^{2n}} + \frac{\hbar^2 k^2}{2m}$$

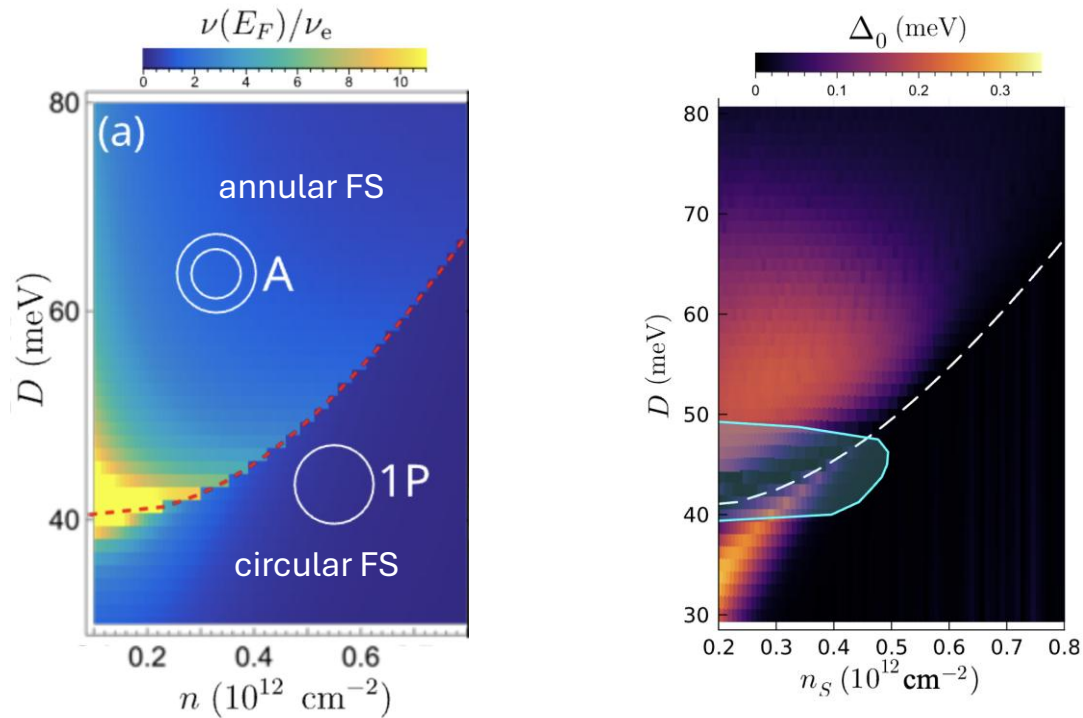
Phase Diagram



Experimental T_c : 200 - 300 mK

p-wave SC from charge fluctuation calculated by RPA.

Topology



circular FS: topological $p + ip$ SC

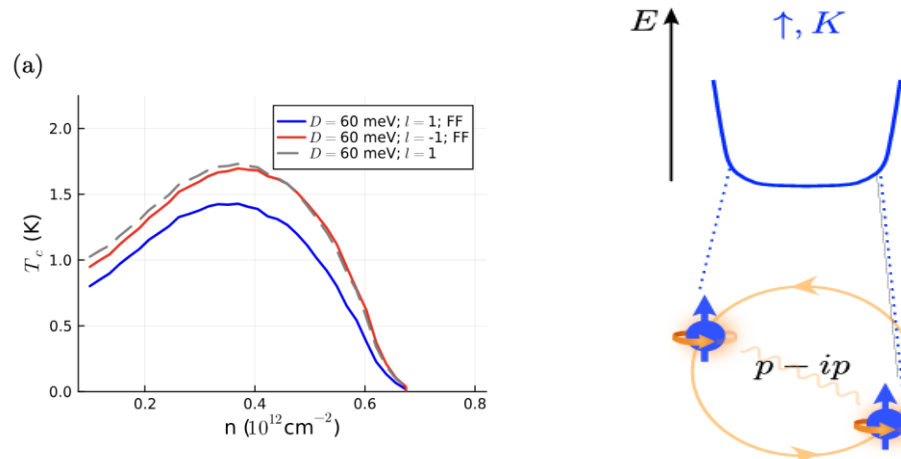
annular FS: trivial $p + ip$ SC ($C=1-1=0$)

$p + ip$ versus $p - ip$

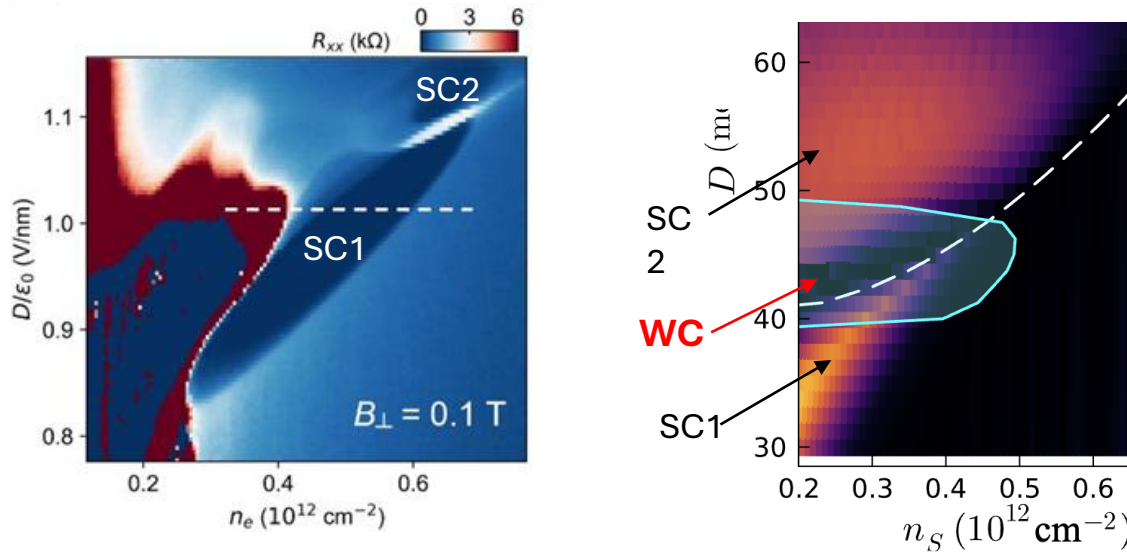
$$\tilde{H}_{int} = \frac{1}{2} \sum_{\mathbf{k}, \mathbf{k}', \mathbf{q}} V(\mathbf{q}) \langle u_{-\mathbf{k}'} | u_{-\mathbf{k}} \rangle \langle u_{\mathbf{k}'} | u_{\mathbf{k}} \rangle \tilde{\psi}_{\mathbf{k}+\mathbf{q}}^\dagger \tilde{\psi}_{\mathbf{k}'-\mathbf{q}}^\dagger \tilde{\psi}_{\mathbf{k}'} \tilde{\psi}_{\mathbf{k}}$$

The full interaction contains the form factor associated with intra-unit-cell Bloch wavefunction, which is complex-valued and thus breaks the time-reversal symmetry.

Chiral nature of Bloch wavefunction in a given valley lifts the degeneracy between $p \pm ip$ pairings.

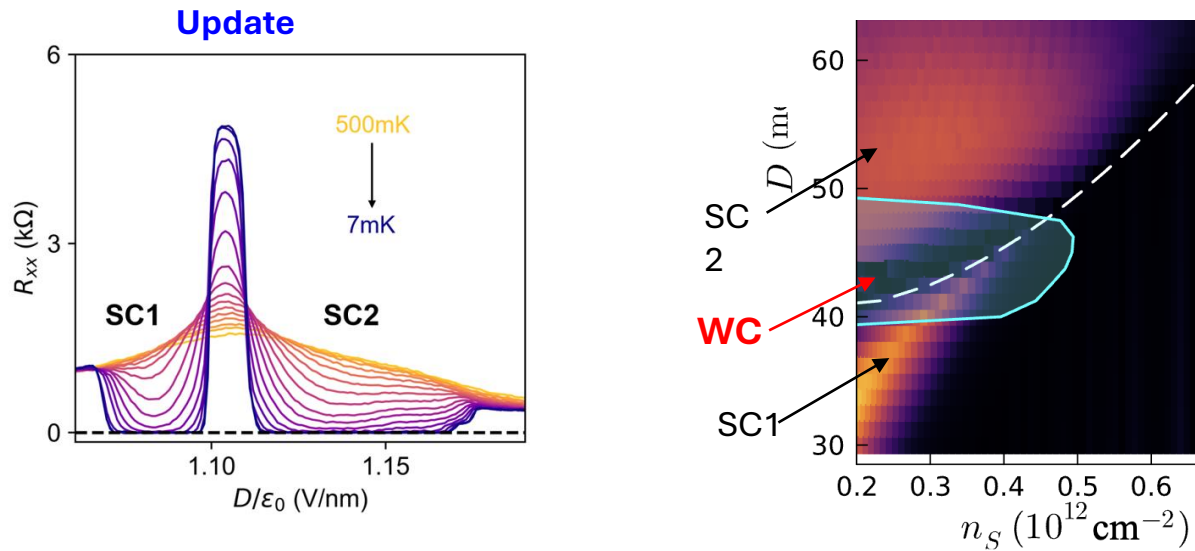


Wigner Crystal Intervening SC1 and SC2



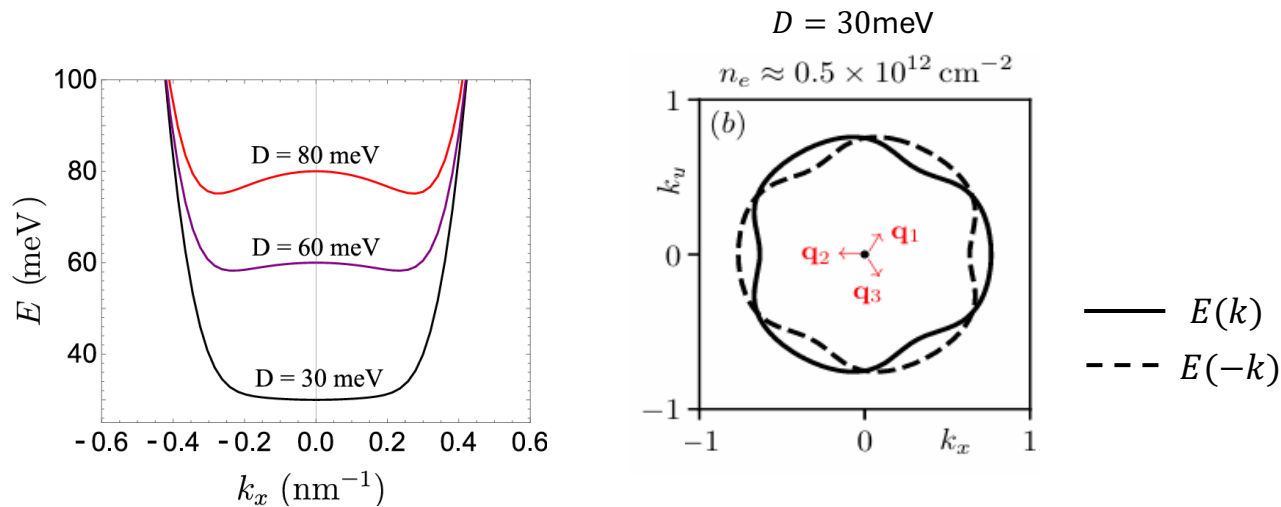
Our analysis suggests Wigner crystal at Lifshitz transition indicated by $E_{\text{int}}/E_{\text{kin}} > 40$, intervening SC1 and SC2.

Wigner Crystal Intervening SC1 and SC2



Our analysis suggests Wigner crystal at Lifshitz transition indicated by $E_{\text{int}}/E_{\text{kin}} > 40$, intervening SC1 and SC2.

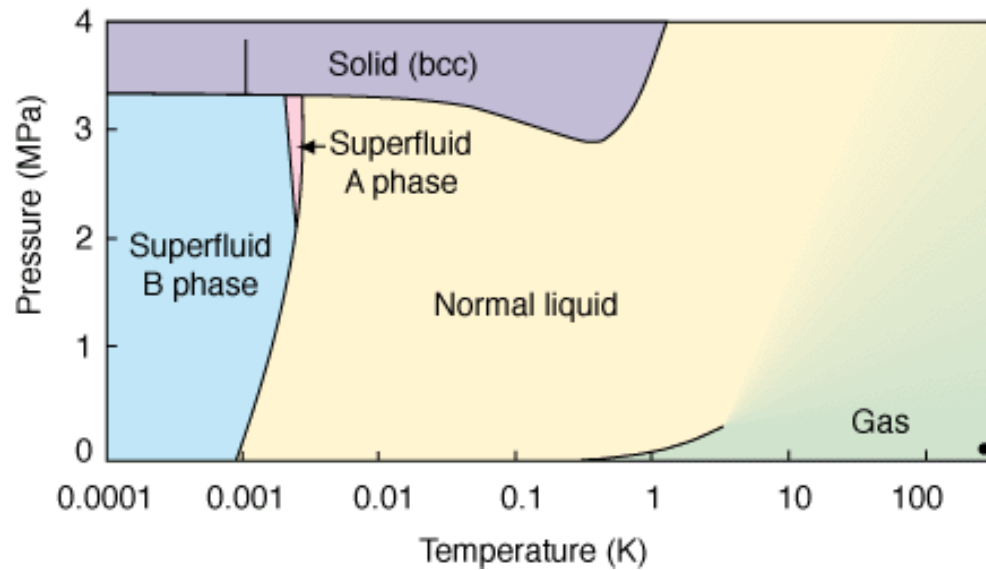
T-Breaking from Trigonal Warping



- $E(k) \neq E(-k)$ within a valley; Cooper log divergence is removed.
- At low density, trigonal warping favors finite-momentum pairing

Model System for Unconventional SC

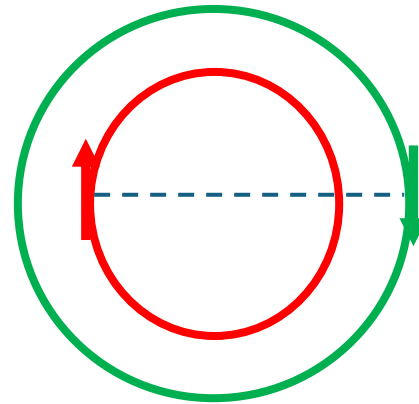
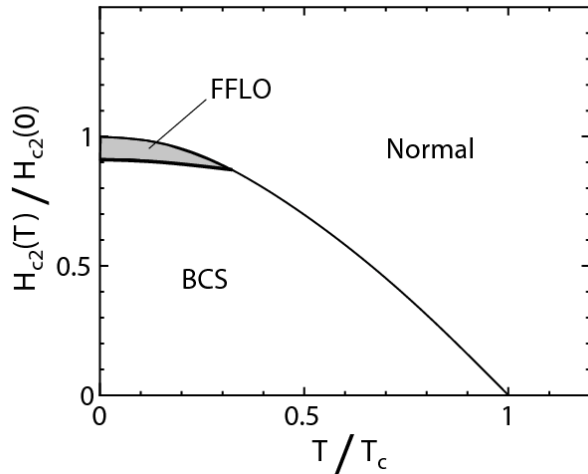
Helium-3: p-wave & topological



Rhombohedral graphene: electronic analog of He-3

Partially Spin Polarized SC

How could spin-singlet SC accommodate spin polarization?

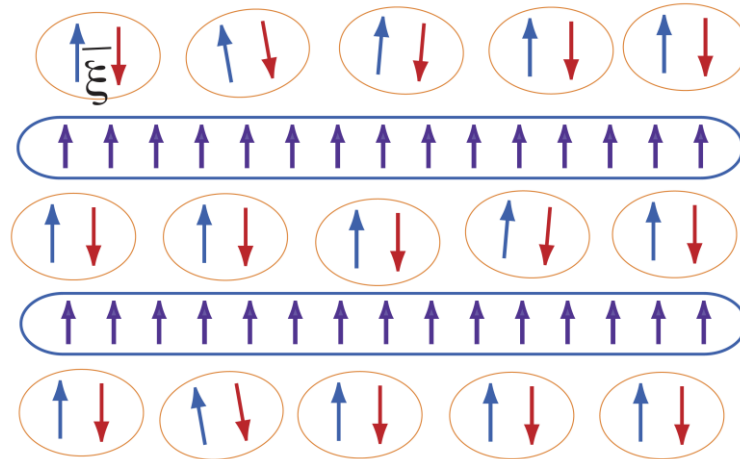


1. $\Delta(\mathbf{r}) = \Delta \cos(\mathbf{q} \cdot \mathbf{r})$ breaking translation symmetry (LO)
2. $\Delta(\mathbf{r}) = \Delta e^{i\mathbf{q} \cdot \mathbf{r}}$ breaking time-reversal symmetry (FF)

FFLO states host singlet pairs and unpaired spin- \downarrow quasiparticles

Pair Density Wave

$$\Delta(\mathbf{r}) = \Delta \cos(\mathbf{q} \cdot \mathbf{r})$$

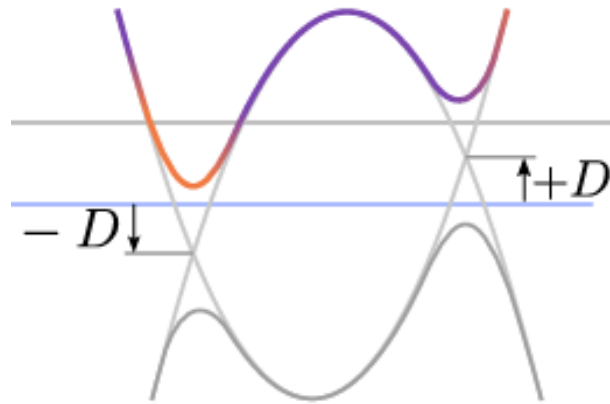


LO states host unpaired spin- \downarrow Andreev quasiparticles at π domain walls.

Finite-Momentum SC

$$\Delta(\mathbf{r}) = \Delta e^{i\mathbf{q}\cdot\mathbf{r}}$$

Doppler shift: $E_k \rightarrow E_k + \mathbf{q} \cdot \mathbf{v}_F$

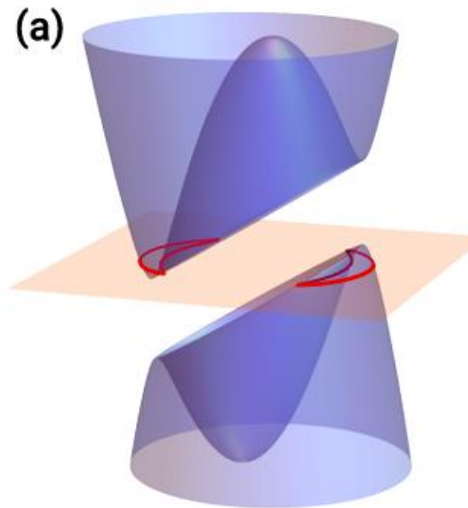


$$H_{\text{MF}} = \sum_k (\epsilon_k - \mu) c_k^\dagger c_k + (\Delta c_{k\uparrow}^\dagger c_{-k+q\downarrow}^\dagger + h.c.)$$

Finite-Momentum (Helical) SC

$$\Delta(\mathbf{r}) = \Delta e^{i\mathbf{q}\cdot\mathbf{r}}$$

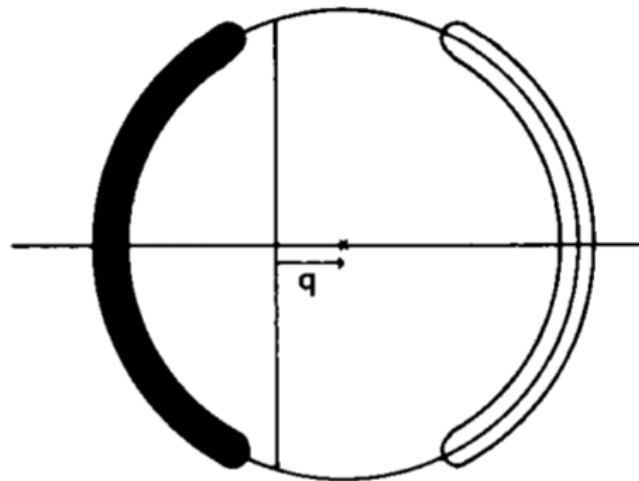
As Cooper pair momentum increases and Doppler shift exceeds the SC gap Δ , unpaired quasiparticles appear in the ground state $c_{\uparrow}^{\dagger} + c_{\downarrow}$ leading to spin polarization.



Bogoliubov
Fermi surface

Tunneling Density of States for a Superconductor Carrying a Current*

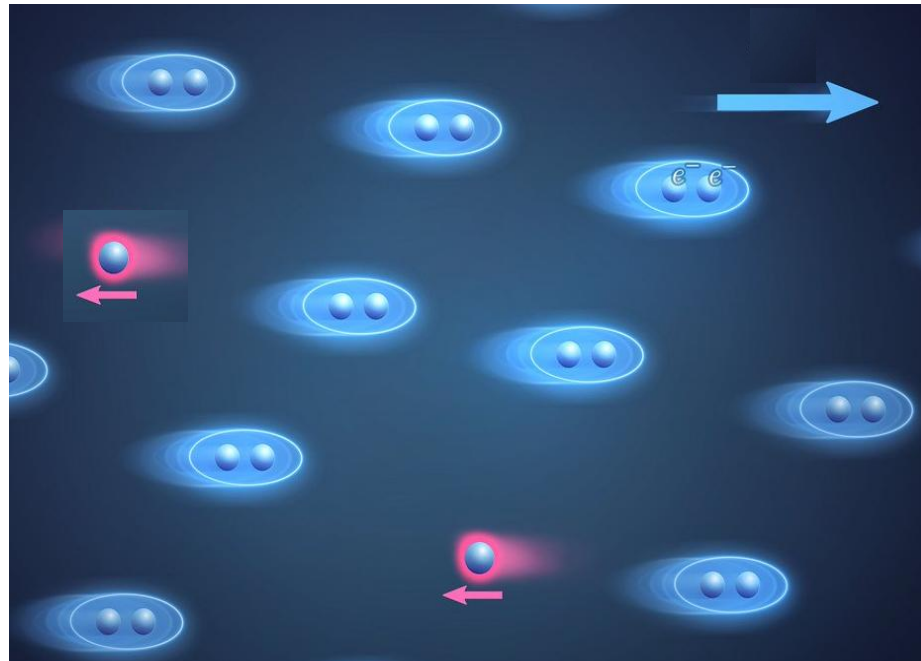
PETER FULDE



- clean limit: gapless SC with segmented Fermi surface

Finite-Momentum Pairing

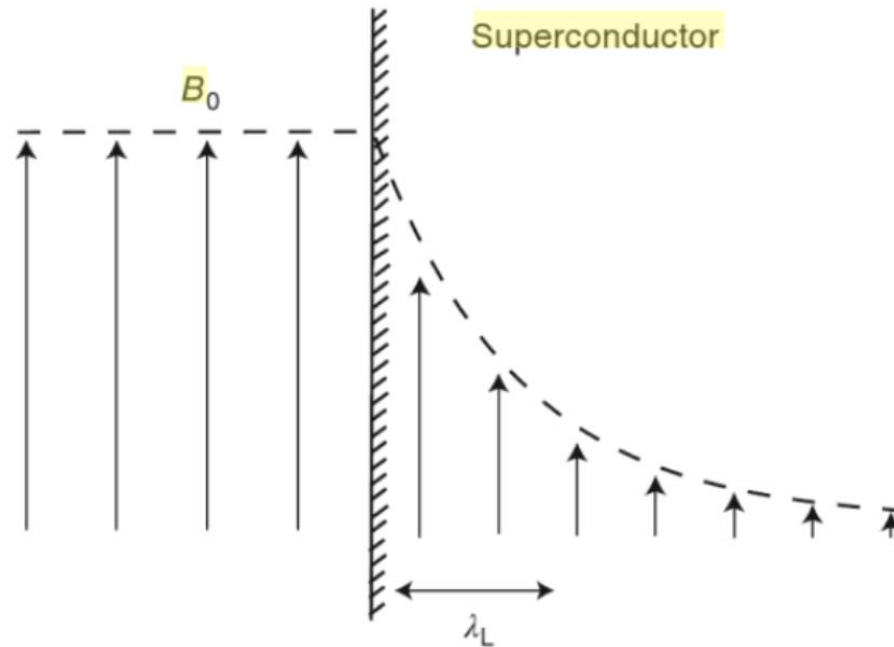
A mechanism for SC diode effect



Cooper pairing at nonzero momentum q allows critical currents parallel and anti-parallel to q to be different.

[Yuan & LF, PNAS \(2021\)](#) see also [Daido, Ikeda & Yanase \(2021\)](#) ...

Finite-Momentum Pairing in Meissner State



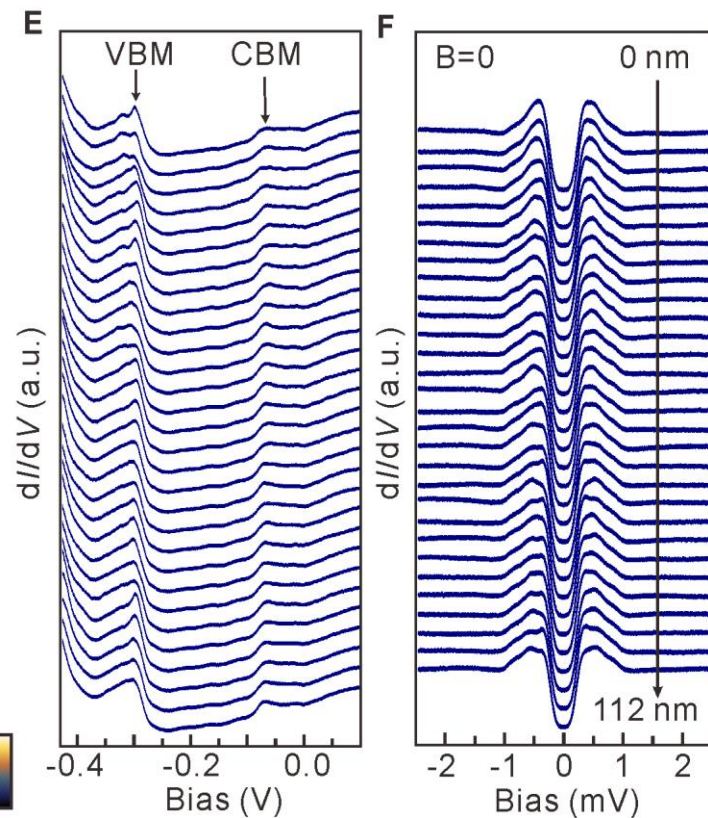
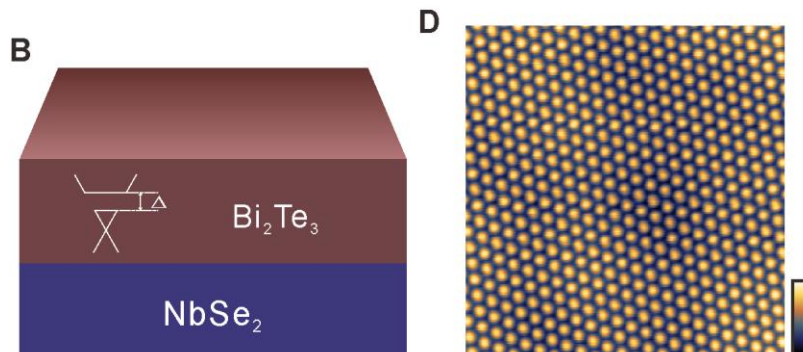
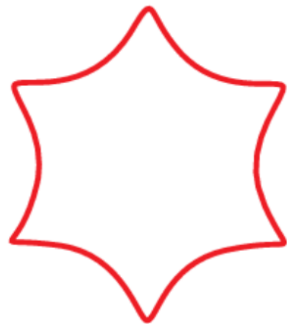
Below H_{c1} , diamagnetic screening current near the surface leads to $\Delta(\mathbf{r}) = \Delta e^{i\mathbf{Q}\cdot\mathbf{r}}$, $Q = eB_0\lambda_L/\hbar$

Superconductor-Topological Insulator: NbSe₂-Bi₂Te₃

Zhu, Papaj ... LF & Jinfeng Jia, Science (2021)

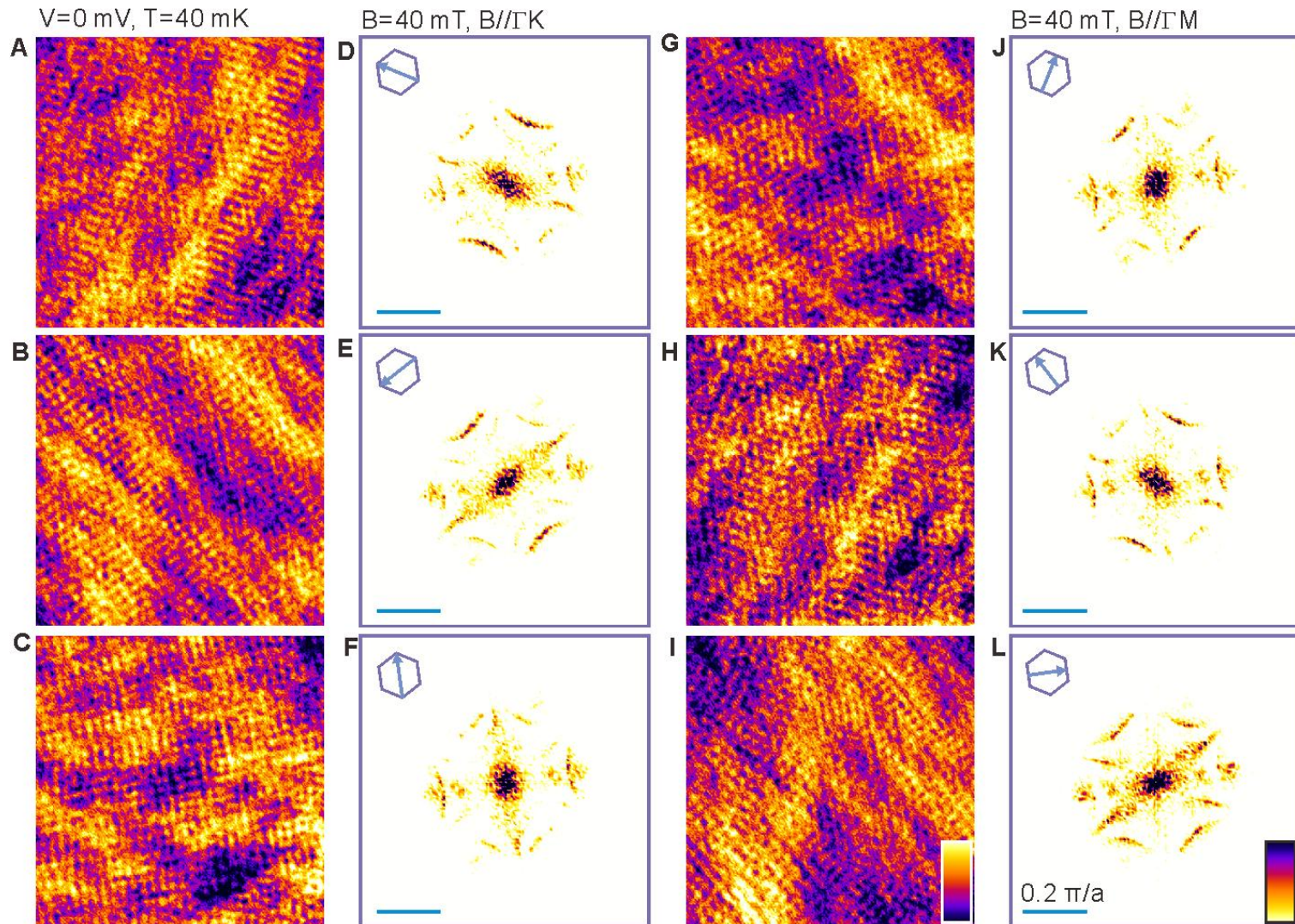
Topological surface state: ▲

Normal FS:

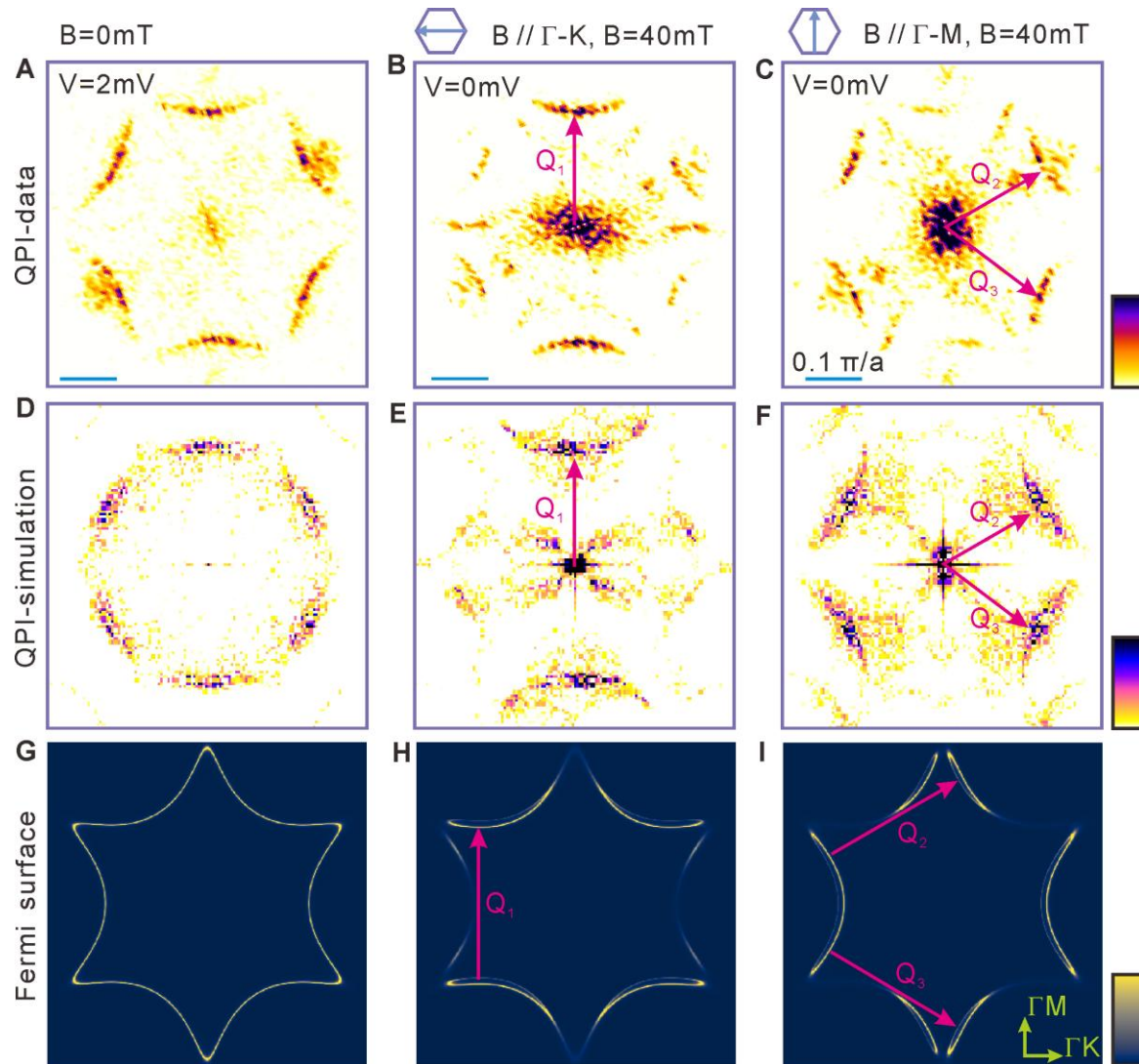


$$H_{c1} \approx 100\text{mT}, \lambda_L \approx 100\text{ nm} \Rightarrow \text{At } 20\text{mT}, Q \approx 3 \cdot 10^{-4} \text{ \AA}^{-1}$$

Quasiparticle Interference Pattern



Quasiparticle Interference Pattern



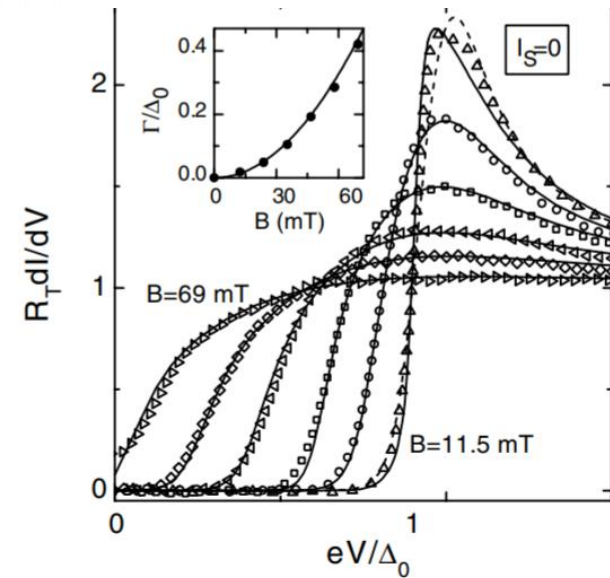
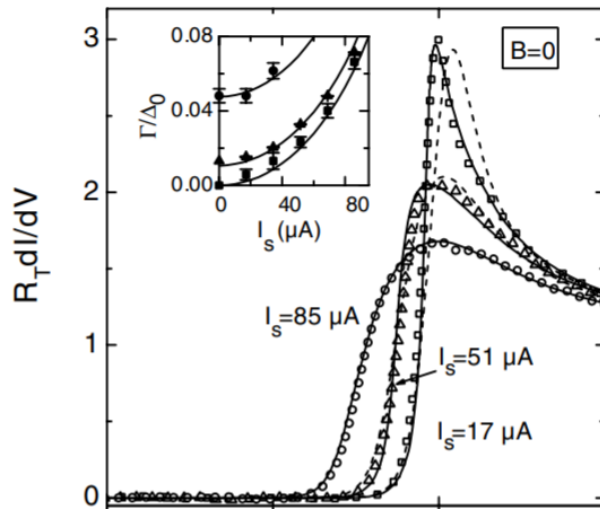
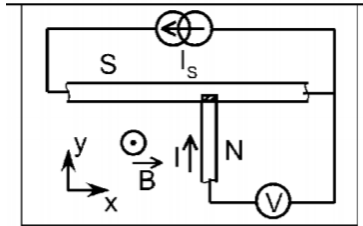
Exotic Forms of Superconductivity

- Excitonic SC
- Spin-polarized SC
- Finite-momentum SC

Density of States in a Superconductor Carrying a Supercurrent

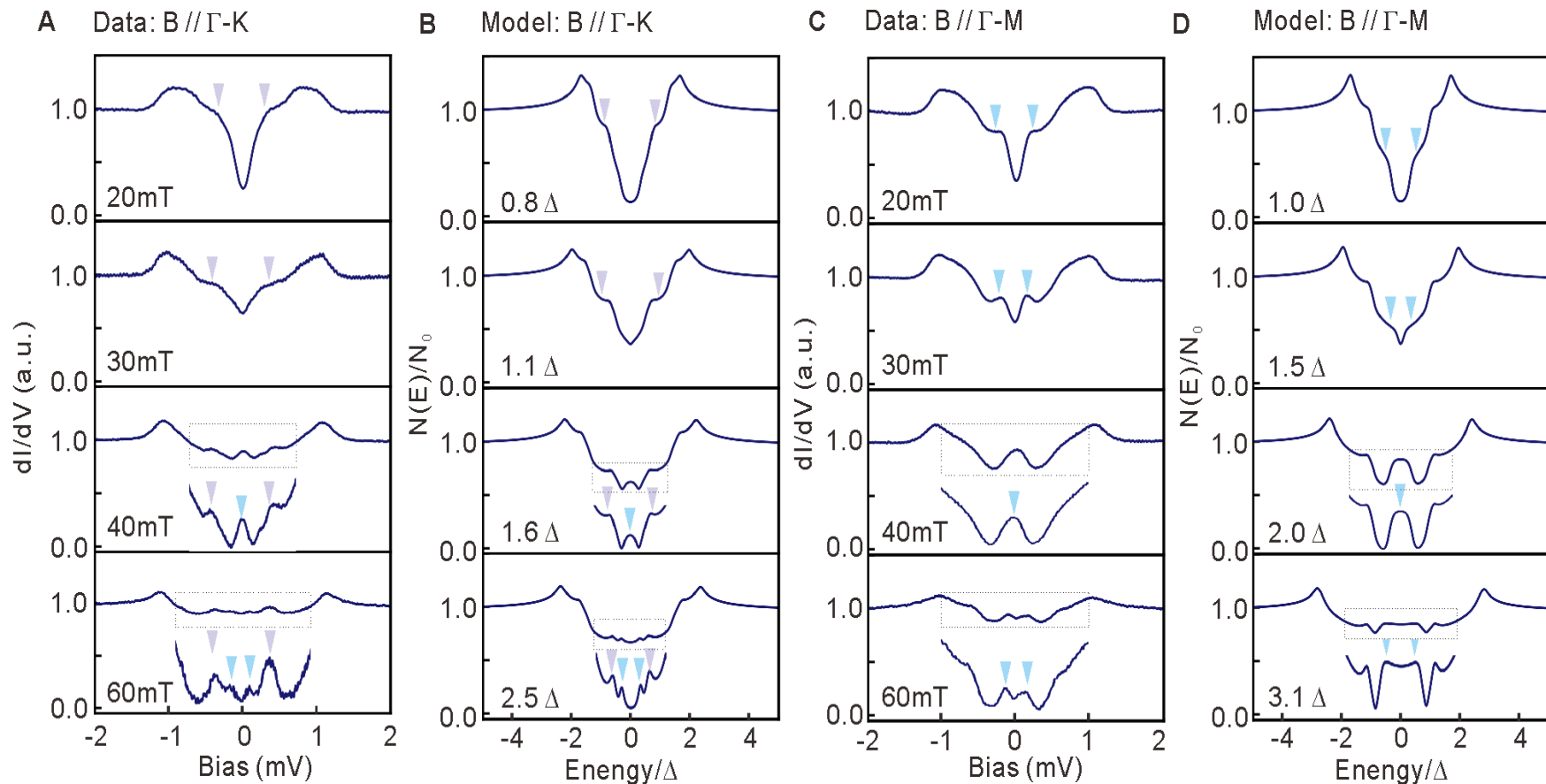
A. Anthore, H. Pothier, and D. Esteve

Service de Physique de l'Etat Condensé, Direction des Sciences de la Matière, CEA-Saclay, 91191 Gif-sur-Yvette, France
(Received 20 December 2002; published 24 March 2003)



- diffusive regime: magnetic field, supercurrent and paramagnetic impurity all have same pairing-breaking effect

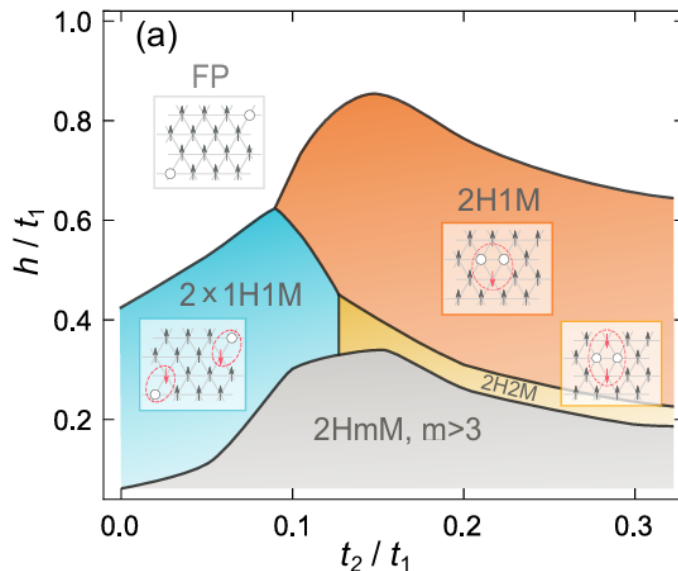
Tunneling Density of States



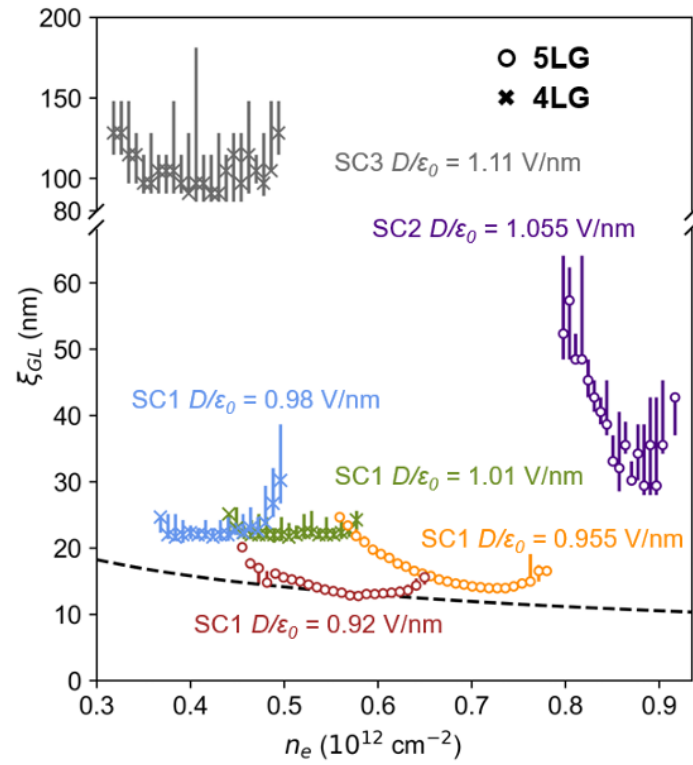
Magnonic Superconductivity

Electron pairs bind with spin-flip (magnon) and condense to form exotic superconductivity with incomplete spin polarization.

$$\langle c_{i\alpha}^\dagger c_{j\beta}^\dagger \rangle = 0 \quad \langle c_{i\uparrow}^\dagger c_{j\uparrow}^\dagger c_{k\uparrow}^\dagger c_{l\downarrow} \rangle \neq 0$$



In this SC, the spin polarization is locked to the doping density, and therefore shows a plateau in $M(H)$.



Gap Structure

Assuming attractive interaction $\sum_{k,k'} V_{kk'} c_{k'}^+ c_{-k'}^+ c_{-k} c_k$:

Mean field gap equation:

$$H_{\text{MF}} = \sum_k (\epsilon_k - \mu) c_k^+ c_k + (\Delta_k c_k^+ c_{-k}^+ + h.c.)$$

with $\Delta_k = \sum_{k'} V_{kk'} \langle c_k^+ c_{-k}^+ \rangle$ and $N = \sum_k \langle c_k^+ c_k \rangle$

Quasiparticle spectrum:

$$E_k = \sqrt{(\epsilon_k - \mu)^2 + \Delta_k^2}$$

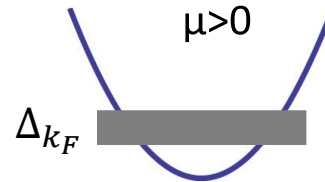
BCS Regime

For weak attraction,

- μ reduces to Fermi energy in normal state.
- $\Delta_{k_F} \ll \mu$
- Coherence length $\frac{v}{\Delta} \gg d$ (interparticle distance)

Quasiparticle spectrum:

$$E_k = \sqrt{(\epsilon_k - \mu)^2 + \Delta_k^2}$$



- $\Delta_k \propto k_x$: anisotropic & nodal (nematic SC)
- $\Delta_k \propto k_x \pm ik_y$: time-reversal breaking & full gap (chiral SC)

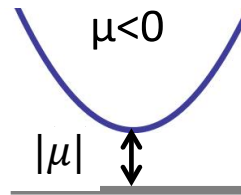
BEC Regime

For strong attraction, tightly bound 2e molecules Bose condense into a superfluid, in which the pairing gap is large compared to noninteracting Fermi energy.

A mean-field description of this BEC state is obtained when μ lies below the band bottom.

Quasiparticle spectrum:

$$E_k = \sqrt{(\epsilon_k - \mu)^2 + \Delta_k^2}$$



- full gap regardless of the pairing form Δ_k

Topology

BCS and BEC phases of a p-wave SC can be *topologically* distinct, in contrast to the case of s-wave SC.

$H_{MF} = \sum_k \Psi_k^+ H(k) \Psi_k$, $\Psi_k^+ \equiv (c_k^+, c_{-k})$ Nambu spinor operator

$$H(k) = \begin{pmatrix} \epsilon_k - \mu & \Delta_k \\ \Delta_k^* & \mu - \epsilon_k \end{pmatrix} \equiv E_k \mathbf{n}_k \cdot \boldsymbol{\sigma}$$

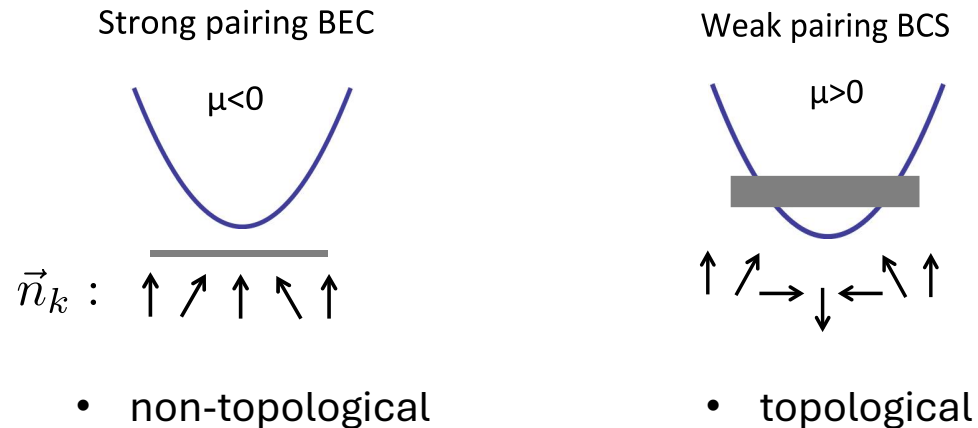
Many-body ground state (=quasiparticle vacuum) is fully determined by “Anderson pseudospin” \mathbf{n}_k .

$$\mathbf{n}_k \cdot \Psi_k |G\rangle = 0 \text{ for all } k$$

Topology

BCS and BEC phases of a p-wave SC can be *topologically* distinct, in contrast to the case of s-wave SC.

1D spin-polarized p-wave SC : Z_2 invariant

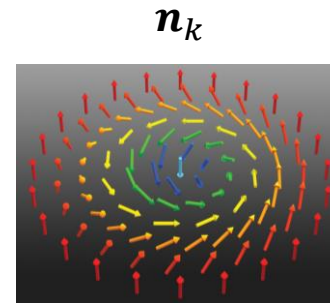
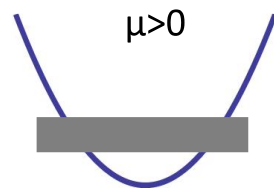


Topology

BCS and BEC phases of a p-wave SC can be *topologically* distinct, in contrast to the case of s-wave SC.

2D spin-polarized chiral p-wave SC:

Weak pairing BCS



Integer Chern invariant N defined by \mathbf{n}_k , mapping from torus to sphere

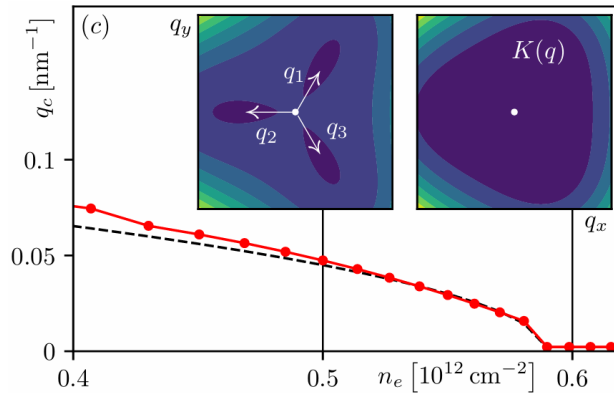
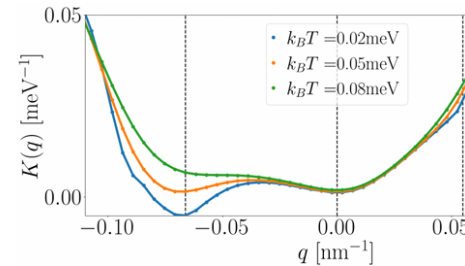
Ginzburg-Landau Theory

GL free energy:

$$F_s = \int d^2\mathbf{r} \left[\alpha(T)|\psi|^2 + \frac{\hbar^2}{2m^*} |\mathbf{D}\psi|^2 + \eta |\mathbf{D}^2\psi|^2 + \gamma \psi^* (D_x^3 - 3D_x D_y^2) \psi + \dots \right]$$

$$\equiv \int dq K(q) |\psi_q|^2 + \dots$$

cubic gradient term allowed by $C_3, M_x T$ and broken T



Transition from uniform to spatially modulated SC as electron density is reduced.

Gaggioli, Guerci & LF,
arXiv:2503.16384

Spontaneous Vortex-Antivortex Lattice (VAL)

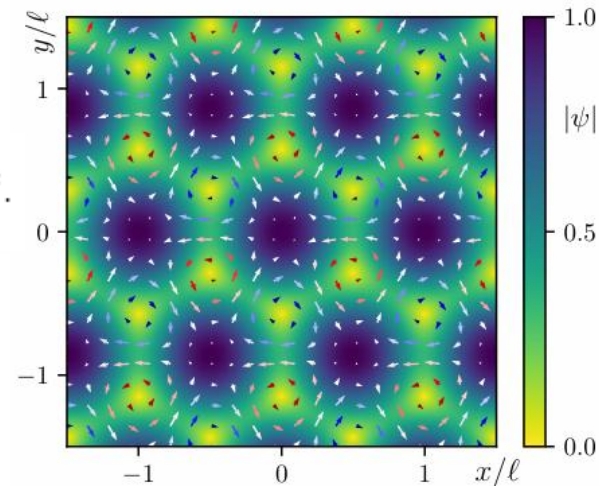
Including quartic terms for Δ_i :

$$f_s = \alpha \sum_{j=1}^3 |\psi_j|^2 + \beta \sum_{j=1}^3 |\psi_j|^4 + \beta' \sum_{i \neq j} |\psi_i|^2 |\psi_j|^2.$$

Microscopic calculation shows

$$\beta > \beta' > 0$$

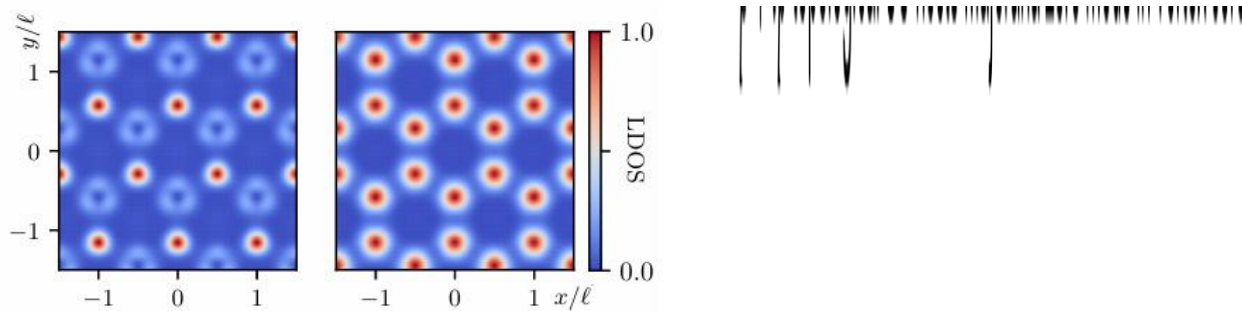
$$\Rightarrow \psi = |\psi_c| (e^{i\mathbf{q}_1 \cdot \mathbf{r}} + e^{i\mathbf{q}_2 \cdot \mathbf{r}} + e^{i\mathbf{q}_3 \cdot \mathbf{r}})$$



Finite-momentum SC state is triple- q pair density wave, exhibiting a lattice of vortices and anti-vortices at $H=0$ (typical $l \sim 100\text{nm}$).

Circulating current produces magnetic field $\sim 10^{-4}\text{mT}$

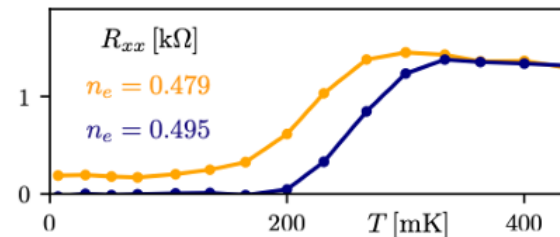
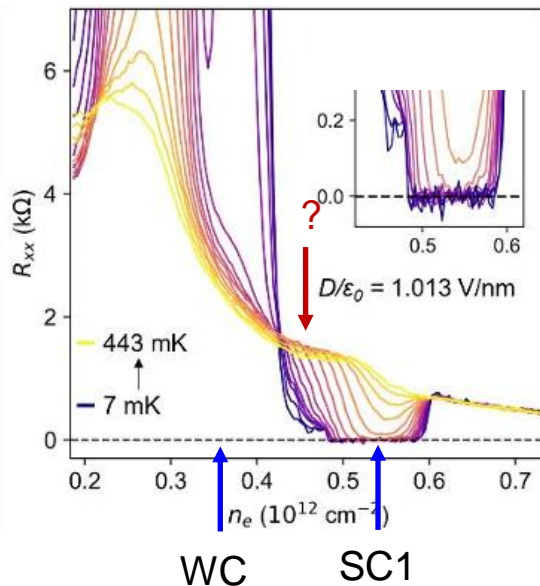
Spontaneous Majorana Fermions



- $p + ip$ topological SC hosts Majorana zero mode in vortex core.
Read & Green (2000), Kraus, Auerbach, Fertig & Simon (2009)
- In VAL state, Majorana fermions residing on honeycomb lattice form low-energy bands
- Topological entropy $2 \log \sqrt{2}$ per unit cell \Rightarrow Pomeranchuk effect

Gaggioli, Guerci & LF, arXiv:2503.16384

Hint of Spontaneous Vortices & Antivortices?

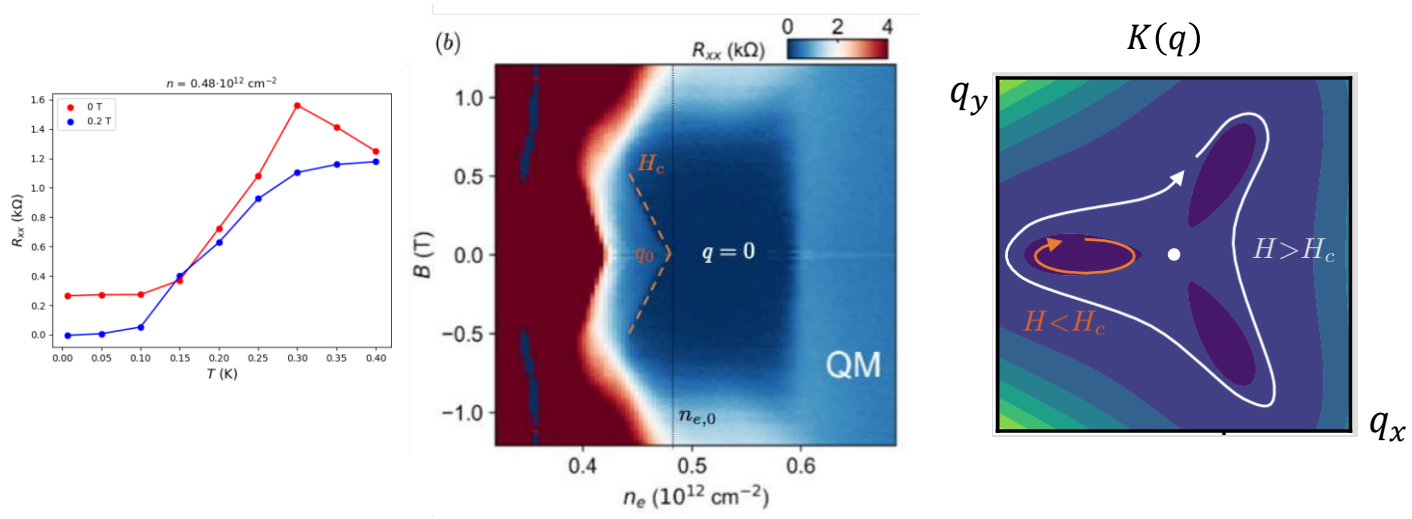


We note an “anomalous” region between SC1 and WC: resistance drops below $\sim T_c$ and saturates to $\sim 10\% R_N$.

We attribute it to flux flow associated with “anomalous” vortices & antivortices.

Analogy with Bardeen-Stephen theory: $R/R_N \sim (q\xi)^2$ around 5-10%.

Magnetic Field Response



Phase transition from $q \neq 0$ to $q = 0$ state induced by small out-of-plane magnetic field $H_c \sim \Phi_0 q_0^2 \ll H_{c2} = \Phi_0 / 2\pi\xi^2$. This explains the phase boundary between SC1 and putative VAL under H.